

How colloidal suspensions that age are rejuvenated by strain application?

Virgile Viasnoff, Stéphane Jurine, and François Lequeux
L.P.M UMR7615 CNRS ESPCI 10 rue Vauquelin 75231 Paris, France
 (Dated: March 22, 2022)

We present here a microscopic study of the effect of shear on a dense purely repulsive colloidal suspension. We use Multispeckle Diffusing Wave Spectroscopy to monitor the transient motions of colloidal particles after being submitted to an oscillatory strain. This technique proves efficient to record the time evolution of the relaxation times distribution. After a high oscillatory shear, we show that this distribution displays a full aging behavior. Oppositely, when a moderate shear is applied the distribution is modified in a non trivial way. Whereas high shear is able to erase all the sample history and rejuvenate it, a moderate shear helps it to age. We call this phenomena *overaging*. We demonstrate that overaging can be understood if the complete shape of the relaxation time distribution is taken into account. We finally report how the Soft Glassy Rheology model accounts for this effect.

PACS numbers: 07.60.-j, 78.35.+c, 81.40.Cd

I. INTRODUCTION

The study of dense colloidal suspensions still raises many open questions. One interesting feature is that some of these systems remain out of equilibrium for any accessible experimental time. For instance, if the pair potential of interaction has an attractive part, the particles can aggregate in an always evolving physical network [1]. If the potential is purely repulsive, an increase of concentration leads to a jamming transition and the suspension can reach an amorphous state or glassy phase [2]. More precisely, in this last case the characteristic relaxation time of the system increases dramatically around a critical value of the volume fraction ϕ_c . For large enough concentrations, the relaxation processes rapidly become longer than any experimental time. The system is then macroscopically pasty and can display a non-stationary behavior. A direct consequence of the extremely long relaxation times is that all the past history of the sample has to be taken into account. A key trick to obtain reproducible results is to perform experiments on a sample with the exact same history. As far as rheological measurements are concerned, it is known for long that a high preshear can erase all past memories in many systems. It is thus often used as a trick to reset the sample history provided that it does not damage it irreversibly. This procedure is reminiscent of the process of thermal quench used to erase the history for other structural or spin glasses [3, 4]. This similarity let envision a comparable role played by shear and temperature on a microscopic level. It has recently been shown on different 'pasty' colloidal suspensions that their macroscopic behavior after a rheological quench have the same qualitative feature than other glasses after a temperature quench [5, 6]. However, measurements of the effect of shear on the dynamic at a microscopic level are still lacking. In this paper we study a colloidal glass with Multispeckle Diffusing Wave Spectroscopy (MSDWS), monitoring the motions of the colloidal particles after that the sample underwent various strain histories. We will show that

the mechanical perturbation acts in a dual fashion on the microscopic dynamic. All the observed effects will be discussed within the Soft Glassy Rheology (SGR) model [7, 8, 9].

II. BACKGROUND

In this section we will recall some general results on glasses. We will mainly focus on results obtained on spin and structural glasses upon a change of temperature. However, most of these results are similar to that observed in colloidal glasses if a temperature decrease is substituted by an increase of concentration [2, 10]. Spin and molecular glasses display a qualitative change in their microscopic dynamic when the temperature is lowered around the glass transition temperature. Actually, the distribution of relaxation times splits into two distinct families when the temperature is decreased (see eg :[2, 11]): on the one hand, short distance motions and vibrations of the particles can be describe by fast individual modes called β modes. Their sensitivity to temperature changes is weak. On the other hand collective motions i.e. structural relaxations, occur through a broad distribution of very slow modes called α modes. This modes are very sensitive to temperature changes. In general, the characteristic time of the α relaxation exhibits such a huge increase when the temperature is lowered, that it seems to diverge, up to experimental evidence. For low enough temperatures, such that the relaxation time is larger than the experiment time by many orders of magnitude, the systems present some strange non-equilibrium features. One of the most striking among them, is the so called aging phenomena. It consists in a drift of the α relaxation time distribution, towards longer and longer relaxation times. This distribution keeps on evolving for any experimental time scale. The simplest way to characterize this drift is to perform a quench from a high temperature state where an equilibrium distribution can be achieved to a low temperature state in the glassy re-

gion [3, 4]. In this case, the age of the system is defined as the time elapsed since the quench, i.e. the time spent in the glassy phase. In these conditions, it has been proven theoretically and experimentally alike that any measured quantities depends explicitly on the age of the system [3]. More precisely, the response and correlation functions do not only depend on the elapsed time t since the beginning of the measurement as it would be the case for an equilibrium system but they also depend on the age of the system t_w , at which the measurement started. Consequently, any correlation function g writes $g(t_w, t + t_w)$. Predictions and experimental results show that, despite the absence of equilibrium, there is a regime often called asymptotic regime, where the only relevant time scale is the very age of the system. As a consequence response or correlation functions can be rescaled with t_w . One finds that $g(t_w, t + t_w) = g(\frac{h(t+t_w)}{h(t_w)})$ where h is a function that depends on the system [12]. When $g(t_w, t + t_w) = g(\frac{t}{t_w})$, the scaling is usually called full aging. We point out, that the existence of such a rescaling in this asymptotic regime shows that the distribution of relaxation times drifts in a self-similar way. Such an asymptotic regime can only be reached if the system is left at a constant temperature for a sufficiently long time in the glassy phase. However, if some additional energy is transiently provided to the aging system, the dependance of the relaxation functions with the age of the system becomes extremely intricate. For example, temperature ramps with stops lead to the very remarkable "memory effect" as observed in spin glasses - see eg [13] - and recently in polymer glasses [14]. The shape of the relaxation times distribution is then modified in a non-trivial way during potentially very long transient regimes. The analysis of this behavior would help to understand the precise modification of the relaxation time distribution by external parameters, and thus to get an insight of the system's internal dynamics. This is the scope of this paper. We have chosen to work on a colloidal glass where it is easy to measure a time-dependant correlation function.

For colloids, temperature is not a practical parameter. But since it is believed that temperature and shear may act similarly in these systems [15], we studied the influence of the shear upon the microscopic dynamics of a colloidal suspension.

In this paper we will focus on the modification of the shape of the distribution of α relaxation times $P(\tau_\alpha)$. We will show that injecting transiently some mechanical energy into the system modifies the distribution of relaxation times in a dual fashion. Conversely to what could be intuitively expected, it can both rejuvenate or *overage* the system. In practice, we study a dense suspension of purely repulsive polystyrene beads both electrostatically and sterically stabilized. We record the fluctuations of a laser light, multiply scattered by the sample. We compute the two times intensity autocorrelation function $g_2(t + t_w, t_w)$. The variation of g_2 is directly related to the mean square displacement of the scatterers.

In order to "quench" the system properly, the sample is first presheared by a large oscillatory strain. When the shear is stopped we record $g_2(t + t_w, t_w)$ for evenly spaced t_w . We show that it displays the properties of full aging. Then the sample is submitted to a burst oscillatory strain of different amplitude and frequency. We monitor the change in the shape of g_2 and interpret it in terms of changes in the distribution of relaxation times.

III. SAMPLE PREPARATION AND EXPERIMENTAL SETUP

The sample is a commercial suspension of polystyrene spherical beads of diameter 162 nm copolymerized with acrylic acid (1%) that creates a charged corona stabilizing the microspheres. The corona prevents both from aggregation by steric and electrostatic repulsions and from crystallization. The suspension was carefully dialyzed to a polymer volume fraction of $\phi = 50\% \pm 0.5\%$. The volume fraction was determined by drying and was chosen to fulfill the two following criteria:

- The sample has to be concentrated enough so that both α and β modes exist. The amplitude of the β mode must be sufficiently small so that the alpha mode can be accurately measured. The α modes must also display some aging behavior over all the experiment time scale.
- The volume fraction has to be low enough so that the strain is homogeneous, at least on macroscopic length scale all through the sample. We checked that no effect like shear banding occurs for the concentrations in use.

Because of the divergence of the viscosity with the volume fraction in the vicinity of the glass transition, the suitable range of concentration fulfilling these two requirements is narrow (between 50% and 52%).

Fig 1 shows the experimental setup. The sample is illuminated using polarized light from an argon-ion laser operating at a wavelength of $\lambda = 514$ nm. The laser beam is expanded to a diameter of approximately 1 cm and is incident on the sample cell. Multiply scattered light is collected by a 50-mm Nikon camera lens and split into two parts. The first part is focused onto an iris diaphragm. The lens is set up so that a one-to-one image of the scattered light from the output plane of the sample cell is formed on the diaphragm. The scattered light emerging from the diaphragm is detected by a Dalsa CCD camera, model CAD1-128A, which is placed approximately $d \simeq 15$ cm behind the diaphragm. It is an 8-bit camera which we run at 500 frames per second. The images are transferred to a computer running at 500 MHz using a National Instruments data acquisition board, model PCI1422. The combined speeds of the computer and data acquisition boards are sufficiently high to allow data to be analyzed in real time. The accessible times range from 10^{-3} s to 10^4 s.

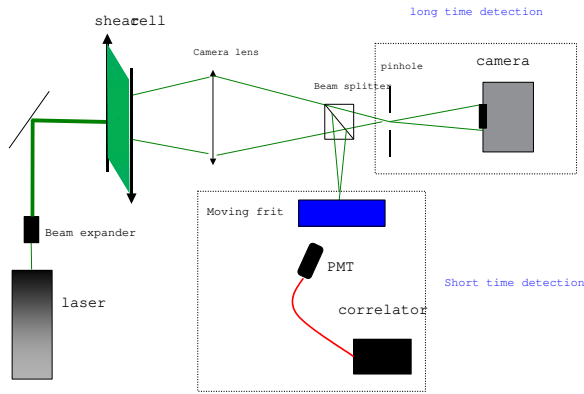


FIG. 1: Experimental set-up. The sample is placed in a shear cell. The emerging light is simultaneously analyzed by the fast correlator and the camera. The problem of ergodicity is solved by performing a spatial average for the camera part, and moving a frit glass in front of the PMT detector for the fast detection.

The second part of the light is shone onto a moving frit. Its motion is controlled by a piezo actuator. The light emerging from the frit is detected by an optical fiber, amplified by an ALV photomultiplier tube (PMT) and analyzed by a Flex correlator. The moving frit has the same effect as the second cell in the two cells technique [16] but we found it easier to implement. It allows an exact determination of the non ergodic correlation function at very short times ($10^{-8}s, 10^{-1}s$). A complete description of the technique can be found in [17]. In the transmitted geometry the correlation functions calculated with the camera and with the PMT can be overlaid [17, 18]. The dynamics of the beads can thus be probed over 12 decades in times. The sample is placed in a custom-made shear cell consisting in two parallel glass plates with a variable gap. For all presented experiments, the gap was set to 1.3 mm. Oscillatory straining was realized by moving the bottom plate thanks to a piezoelectric device. Shear strain from 30% to 0.04% could be possibly applied at different frequencies ranging from 0.01Hz to 10Hz.

IV. EXPERIMENTS

A. rheological quench

In order to check if an oscillatory strain is able to entirely rejuvenate the sample, we submitted the suspension to a series of shear strain of different amplitudes at a fixed frequency of 1Hz for 100s. The measurement of the correlation function starts when the strain is stopped (see fig 2a). The shear cessation is taken as the origin for the age t_w of the system. For a strain amplitude above 20% the correlation functions become insensitive to the strain

amplitude and to the past history. A reproducible state is reached. We have checked that this state does not depend on the duration of the strain application provided that it is superior to 40s. Typical curves are plotted on fig 2b for a volume fraction of 51%.

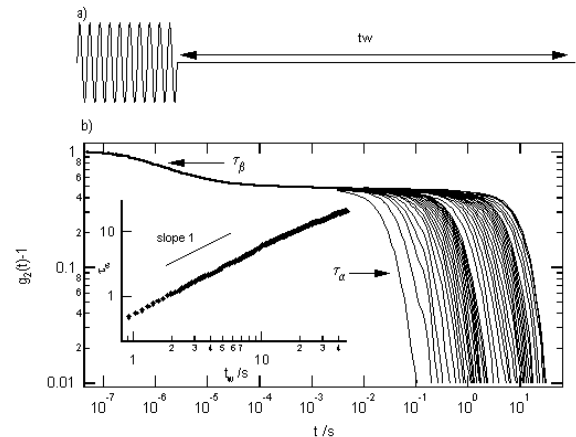


FIG. 2: Normalized intensity autocorrelation functions. The fast decrease of the function corresponds to the β modes and is measured via the correlator. The long time decay corresponds to the α modes -structural rearrangements. It never reaches any steady state on our experiment time scale. The β modes are insensitive to shear and are in a steady state. For sake of clarity only one curve was plotted for the short times. Inset: τ_α versus t_w . We find that the relaxation time varies linearly with the waiting time.

The correlation function shows a characteristic two steps decay as earlier mentioned. A first decrease happens around $\tau_\beta = 10^{-6}s$. It is insensitive to shear (for sake of clarity only one curve has been plotted). Then the correlation function plateaus at a value $g_{plat} \simeq 0.5$. We use a regular algorithm to extract the mean square displacement of the beads for this plateau value. It corresponds fluctuation of position over a distance of $\delta \simeq 9nm$. Finally a second decrease takes place at a time τ_α that varies with the age of the system. τ_α is arbitrarily defined so that $g(t_w, t_w + \tau_\alpha) = \frac{1}{2}g_{plat}$. The inset of fig 2 shows that τ_α evolves proportionally with the sample's age t_w . All the aging part of the curve can be rescaled by t/t_w as displayed on fig 3. The aging part displays thus the characteristic scaling of full aging. It means that $P(\tau_\alpha)$ evolves in a self-similar manner. The high shear provided the system enough energy to entirely rejuvenate it. It thus corroborates the macroscopic observations previously mentioned. It also emphasize the analogy between temperature and strain as far as quenches are concerned.

B. Effect of a moderate oscillatory shear

We now examine the influence of the strain amplitude upon the microscopic dynamics. All the following curves

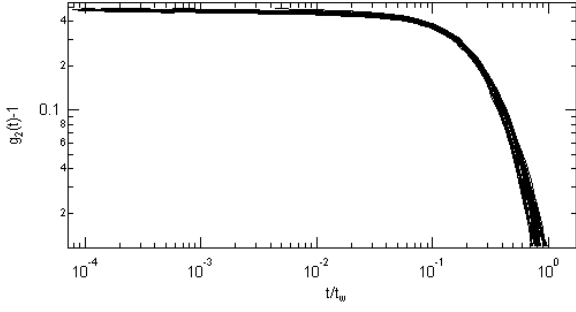


FIG. 3: α relaxation of the intensity autocorrelation function vs $\frac{t}{t_w}$. The rescaling of the curves is satisfactory.

are taken in backscattering geometry for a volume fraction $\phi = 50\%$ and a measured value of $\delta \simeq 68\text{nm}$. As demonstrated in the previous section, a high shear is able to entirely rejuvenate our system. Hence we first submit the sample to an oscillatory strain of 30% for 100s in order to obtain reproducible results. Secondly, the system is left at rest for 10s then it is submitted to a second burst of oscillatory strain of different amplitude γ_0 and duration du . We set the frequency to 1Hz. The strain history is displayed on fig 4a. We now take the origin of the system's age just after the **second** burst. This convention is purely arbitrary but it allows an easier representation of our results on a log scale. We record $\tau_\alpha(\gamma_0, t_w)$ as a function of t_w for different amplitudes of γ_0 . We take the curve for $\gamma_0 = 0\%$ as the reference curve. On fig 3b we plotted the ratio $R = \tau_\alpha(\gamma_0, t_w)/\tau_\alpha(0, t_w)$. If $R < 1$, then the effect of shear is to rejuvenate the system, that is to say that the sheared sample has a quicker dynamics than the unperturbed one. If $R > 1$, then the internal dynamics is slowed down by the shear application. We call this situation "overaging". If a single oscillation is applied at 1Hz for 1s, the sample is partially rejuvenated whatever the strain amplitude may be. This is shown on fig 4b where all the curves lie in the region where $R < 1$. One can wonder if the partial rejuvenation corresponds to a simple backward shift of $P(\tau_\alpha)$. In other words, does the rejuvenation process under shear is the time reversal process of aging? If this would be the case, one could define an effective age t_{eff} such that $\tau_\alpha(\gamma_0, t_w + t_{eff}) = \tau_\alpha(0, t_w)$.

Experimentally we could not find such an effective age and time translation proved inefficient to collapse all the $\tau_\alpha(\gamma_0, t_w)$ onto a master curve. It thus mean that $P(\tau)$ is not modified by the strain in a self-similar manner. However, at long t_w all the curves merges to $R = 1$, indicating that at long times the self-similarity is recovered as expected.

However if 100 oscillations are applied for 100s at 1Hz, the situation is changed as shown on fig 4c. For the highest shear amplitude the ratio R remains constantly below 1 consistently with the results of the previous section. However for the smallest strain amplitudes, R is

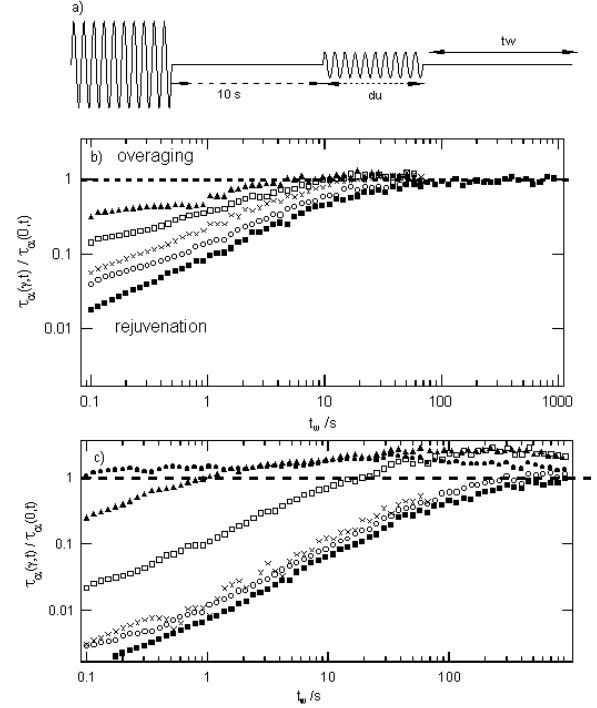


FIG. 4: a) Strain history $\gamma(t)$. We vary both the amplitude and duration of the second burst. b) Normalized relaxation time $\tau_\alpha(\gamma_0, t_w)/\tau_\alpha(0, t_w)$ vs t_w after a burst of duration 1s at 1Hz for different amplitudes $\gamma_0 = 2.9\%$ (\bullet), $\gamma_0 = 5.9\%$ (\blacktriangle), $\gamma_0 = 7.9\%$ (\square), $\gamma_0 = 11.7\%$ (\times), $\gamma_0 = 14.5\%$ (\circ), and complete rejuvenation (\blacksquare). c) Same curves for a duration of 100s. Notice that for the lowest shear amplitude overaging occurs.

first inferior to one but then becomes superior as t_w increases. The effect of shear for this amplitude is thus dual. Shortly after the burst the dynamics is accelerated. But after a while it becomes slower than that of the unperturbed case. It thus means that the transient shear application has modified the distribution of the relaxation times not only in a non self-similar manner but also in a non monotonic way.

Notice, however that at very long times all the curves seem to converge to $R=1$. It shows that regular aging is recovered. By considering only τ_α in the relaxation process we have reduced the relaxation to a single time. However, the shape of the correlation function is the result of the whole distribution of relaxation times. It is thus interesting to compare the full correlation function $g_2(t, t_w, \gamma_0)$ to the reference one $g_2(t, t_w, 0)$.

Fig 5 shows the reference curves $g_2(t, t_w, 0)$ for $t_w = 0.1\text{s}$ (dark line) and $t_w = 60\text{s}$ (grey line). We emphasize the fact that t_w is now referenced from the cessation of the burst. The symbol curves represent $g_2(t, t_w, 7.9\%)$ for $t_w = 0.1\text{s}$ (\circ), $t_w = 1\text{s}$ (\triangle), and $t_w = 60\text{s}$ (\square). The comparison of the curves for $t_w = 0.1\text{s}$ reveals that $g_2(t, t_w, 7.9\%)$ starts decreasing earlier than $g_2(t, t_w, 0\%)$. It is thus an indication that faster re-

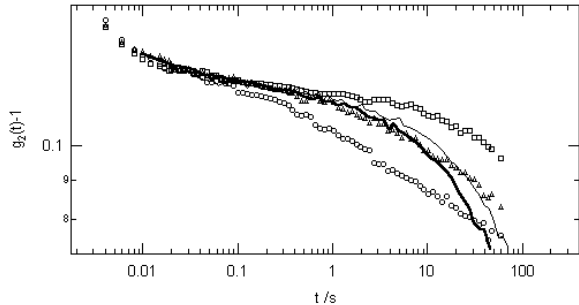


FIG. 5: Correlation functions obtained after the second burst in the reference case for $t_w = 10^{-1}s$ (Bold line) $t_w = 60s$ (Grey Line) and in the case $\gamma_0 = 5.9\%$ for $t_w = 10^{-1}s$ (O), $t_w = 1s$ (Δ), $t_w = 60s$ (\square). Notice the crossing of the curves occurring around 30s. The change in the shape of the correlation function is clearly visible.

laxation process occurs in the sample. However, at long times, $g_2(t, t_w, 7.9\%)$ crosses and then lies above $g_2(t, t_w, 0\%)$. It thus means that at long times the relaxation processes in the sheared sample are slower than in the reference one. This is confirmed by the relative position of $g_2(t, t_w, 7.9\%)$ and $g_2(t, t_w, 0\%)$ for $t_w = 60s$. $g_2(t, t_w, 7.9\%)$ decreases more slowly than $g_2(t, t_w, 0\%)$. Thus, the fast relaxation times have aged and the dynamics is dominated by the slower ones. The change in the shape of the correlation function is the very sign that the relaxation time distribution has not been simply shifted backwards in time by a constant amount, but that its shape has been modified with an addition of short and long relaxation times.

C. effect of frequency

Up to now, we have only focused on the amplitude and duration of the second burst. However, one can also expect that its frequency plays a role in the rejuvenation-overaging process. Indeed, one could expect that not only strain but also strain rate is an important factor in this mechanism. We set the amplitude to 7.9% and the duration of the burst to 10s. We varied the frequency from 0.1Hz to 10Hz. Hence the sample was submitted to a number of oscillations n ranging from 1 to 100. The results are displayed on fig 6. Notice that the overaging effect is all the more pronounced that the frequency is high. We believe though that the overaging behavior cannot be observed under steady strain rate as usually performed in rheological measurements. However, we could not check this hypothesis since our set up does not allow continuous straining.

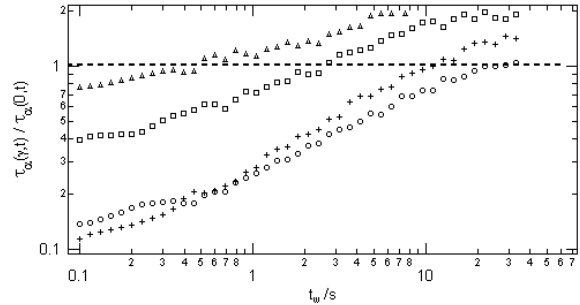


FIG. 6: Normalized α relaxation time for $\gamma_0 = 7.9\%$ at various frequencies: 0.1Hz(\circ), 1Hz($+$), 5Hz (\square), 10Hz (Δ). Notice that the importance of the overaging regime increases with the frequency.

D. experimental conclusion

In conclusion, we have shown that a high shear is able to generate in the system a distribution of relaxation time $P(\tau_\alpha)$ independent of the sample history and of shear amplitude. We then demonstrated that a moderate oscillatory strain both partially rejuvenate and overage the system. We deduced from that point that the rejuvenation process is not a simple backwards time translation of $P(\tau_\alpha)$. It involves a more sophisticated process during which the shape of the distribution is modified. However, independently of the imposed perturbation, $P(\tau_\alpha)$ seems to converge to the same time-dependant distribution at very long times. In addition, if an oscillatory strain is applied similarly but at a higher frequency the overaging process is amplified.

V. SGR MODEL

In a previous paper [19] we emphasized the similarity of this results with the predictions of the simple trap model [20] solved with a step in temperature. This qualitative agreement reinforces the similarity of shear and temperature on the particles level. We also pointed out that a resolution of the Sherrington-Kirkpatrick model for spin glasses in the transient regime following a temperature step gives the same results [12, 21]. However, the equivalence between shear and temperature increase remains an hypothesis. We present here some results on a model where the macroscopic shear is coupled to the microscopic. There are only two of such models that we are aware of. One is based on a mode coupling approach and has only been solved in the asymptotic regime [22]. The other one is inspired from the trap model and is called the Soft Glassy Rheology (SGR) model [7, 8, 9]. We will now solve this model for the transient strain history applied to our system.

The basis of the model are the following: the system is described by fictive independent particles moving in a

fixed energy landscape. Only local minima are considered. The particles are trapped in wells of depth E from which they escape in a "thermal" like fashion. The escaping probability is proportional to $\exp[-E/x]$ where x plays the role of the thermal energy. The macroscopic strain is introduced as an external field that shifts the minimum energy levels E by an amount $-\frac{1}{2}kl^2(t)$ where $l(t)$ is the local accumulated strain. Thus straining helps to hop outside the wells. In order to calculate $l(t)$ the following assumptions are made:

- i. Each time a particle escape from a trap, it falls in an unconstrained state of depth E with $l = 0$. The probability of falling in a trap of depth E is proportional to the density $\rho(E)$ of trap E .
- ii. The strain rate is homogeneous all over the sample.

- iii. The two preceding hypothesis allow to define $l(t)$ as the integrated local strain since the last hopping event t_l for the particle: $l(t) = \int_{t_l}^t \dot{\gamma} dt$.
- iv. The local elastic modulus k is independent of the trap depth.
- v. $\rho(E)$ is exponential: $\rho(E) = \frac{1}{x_g} \exp[-E/x_g]$.

A complete description and justification of the model can be found in [7].

We call $P(E, l, t)$, the time-dependant probability for a particle to be in a well of depth E with a strain l . The evolution of $P(E, l, t)$ in the SGR model reads as:

$$\frac{\partial P(E, l, t)}{\partial t} = - \underbrace{P(E, l, t) e^{-(E - \frac{1}{2}kl^2(t))/x}}_{\text{escaping term}} + \underbrace{\Gamma(t)\rho(E)\delta(l)}_{\text{entering term}} - \underbrace{\dot{\gamma} \frac{\partial P(E, l, t)}{\partial l}}_{\text{external advection}} \quad (1)$$

where the time unit has been set to 1, and with

$$\Gamma(t) = \int_{-\infty}^{\infty} \int_0^{\infty} P(E', l', t) e^{-(E - \frac{1}{2}kl'^2(t))/x} dE' dl'$$

Each (E, l) state is thus associated with a relaxation time $\tau_E \propto \exp[(E - 1/2kl^2)/x]$. In absence of shear, the local strain remains always equal to zero, and the model reduces to the Bouchaud's trap model: for $x > x_g$, a steady distribution for $P(E)$ exists. Oppositely, for $x < x_g$ no steady distribution exist and $P(E)$ reaches an asymptotic regime with a full aging behavior. Subsequently x_g is assimilated to a glass transition temperature. If a constant shear rate is applied, the system always displays an equilibrium distribution of relaxation times. The model describes qualitatively well many rheological features of soft glassy systems [7, 8, 9].

We numerically solve the equation 1 by discretizing the equation into 100 energy levels and 100 strain level. We checked that the obtained results do not depend on the numbers of levels we use. We take $k = 2$, $x_g = 1$ and $x = 0.5$. We remark that the values of γ can not be compared to that really used in the experiments. We use the initial conditions of a deep quench. The system is supposed to have its equilibrium distribution for $T = \infty$. Hence, $P(E, l, 0) = \rho(E)\delta(l)$. The external strain is taken as follows:

$$\gamma(t) = \begin{cases} 0 & \text{if } t < t_{att} \\ f(t) & \text{if } t_{att} \leq t \leq t_{att} + du \\ 0 & \text{if } t > t_{att} + du \end{cases} \quad (2)$$

$f(t)$ is a function of t that will be specified cases by cases. We discuss the effect of shear by computing $P(\varepsilon, t)$ with $\varepsilon = E - \frac{1}{2}kl^2$. Notice that the relaxation time distribution $P(\log(\tau_E)) \propto P(\varepsilon)$. Hence $P(\varepsilon)$ and $P(\tau_E)$ have the same physical meaning. For sake of clarity, we will use $P(\varepsilon)$ for which all the described effects are more visible.

A. one step

Firstly, we exemplify the effect of a single square pulse: $f(t) = \gamma_0$.

We first let the initial distribution $P(E, l, 0) = \rho(E)\delta(l)$ evolves between $t = 0$ and $t = t_{att}$. We chose t_{att} so that $P(E, l, t_{att})$ has nearly its self-similar shape. In this regime, the t/t_w scaling leads to the following property for the distribution function:

$$P(E - e, l, t) = P(E, l, t - t_{eff}) \quad (3)$$

with $t_{eff} = t(1 - \exp[-e/x])$ and e is any positive constant. For $t = t_{att}$, the effect of the step is to shift the states $(E, 0)$ to the states (E, γ_0) .

For $t_{att} < t < t_{att} + du$ the population is now split into two levels as the particles always jump from a (E, γ_0) state to a $(E, 0)$ one. One can show that, because of equation 3, the evolution of $P(\varepsilon, t)$ during the step is the same than that of the unperturbed case but shifted in time by $t_{eff} = t_{att}(1 - \exp[-\frac{1}{2}k\gamma_0^2])$. However, according to equation 1 the states (E, γ_0) do not age but simply becomes depopulated. Only states $(E, 0)$ have a non zero entering rate. Hence there is no possible self-similar regime for

$P(E, l, t)$ until $P(E, \gamma_0) = 0$. Hence at $t = t_{att} + du$ the effect of shear is to shift backwards all the levels: (E, γ_0) states are shifted to $(E, 0)$ and $(E, 0)$ states are shifted to $(E, -\gamma_0)$ states. However, the effect of the strain shift differs from a simple shift in time because $P(E, l, t)$ is not in its self-similar regime - despite the fact that $P(\varepsilon)$ has its self similar shape-.

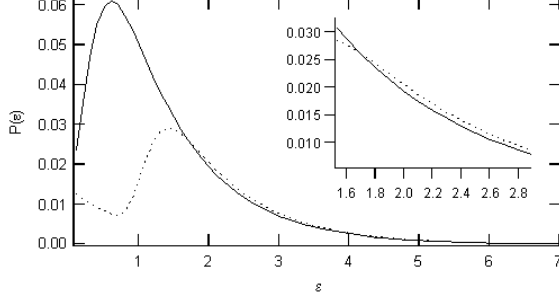


FIG. 7: Distribution function $P(\varepsilon)$ when no shear is applied (stray line) and when a strain square pulse ($\gamma_0 = 0$) is applied. The inset is a zoom on the region where the overaging is visible.

Fig 7 shows that it leads to split of the $P(\varepsilon)$ into two bumps. Low energies are mainly populated by the particles that hopped during the square pulse. Conversely, high energies are mainly populated by particles that did not hop. But in addition, and as a result of the whole history these levels become overpopulated by jumps from the low energy levels. Finally, a splitting of the distribution results from the acceleration of the kinetics of low energy levels and overaging originates from this splitting of the energy population.

Discretizing the strain history as very short steps, one can solve equation 1 for any strain history. We will see in the following section that an oscillatory strain amplifies deeply the splitting of $P(\varepsilon)$.

B. sinusoidal strain

1. effect of amplitude

In this section we take $f(t) = \gamma_0 \sin(\omega t)$ with $\omega = \frac{2}{5}\pi$. It corresponds to a burst of 10 cycles. Fig 8 shows $P(\varepsilon)$ 0.1 tu after the burst.

The solid line corresponds to the unperturbed case: $\gamma_0 = 0$. The curves lie in increasing order of strain amplitude γ_0 from bottom to top on the right hand-side of the figure. It appears that for large amplitudes -eg $\gamma_0 = 4.5$ - the system is accelerated. Indeed, the distribution $P(\varepsilon, 4.5)$ lies over the reference one for small ε i.e. small relaxation times, and below the reference one for large ε i.e. long relaxation times. It thus corresponds to a case where the system was rejuvenated. Interestingly, for moderate amplitudes. The distribution splits

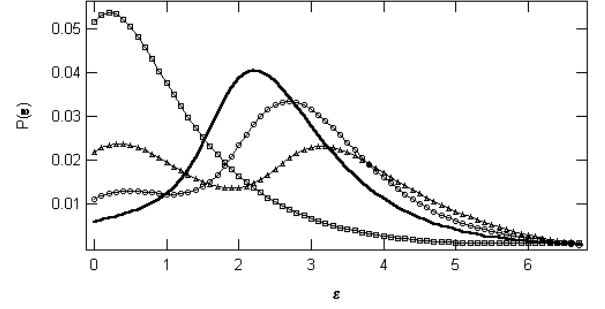


FIG. 8: Calculated distribution $P(\varepsilon)$ at 5Hz for different strain amplitude $\gamma_0 = 0$ (Bold Line), $\gamma_0 = 1.7$ (○), $\gamma_0 = 2.5$ (△), $\gamma_0 = 4.5$ (□). Notice the splitting of the distribution and the surpopulation of both the short and large ε compare to the reference case $\gamma_0 = 0\%$.

into two bumps. Both low and high ε lie above the reference curves, whereas the population of moderate ε are depleted. In order to better understand how the splitting of the correlation function influences the dynamics, we calculated:

$$C(t_w + t, t_w) = \iint_0^\infty P(E', l', t_w) e^{[-t \cdot e^{-(E' - \frac{1}{2} k l'^2)/T}]} dE' dl'$$

$C(t + t_w, t_w)$ is the probability that a particle has not change its position between time t_w and $t_w + t$. It is actually similar to our measured correlation function $g_2(t + t_w, t_w)$. More precisely, g_2 is a monotonic function of C , going from 1 to 0, while C is going from 1 to 0. The detailed shape of $g_2(C)$ depends on the set-up optical characteristics and is of no interest in the following. Optically the situation is similar to the one of structurally evolving foams and is discussed in [23].

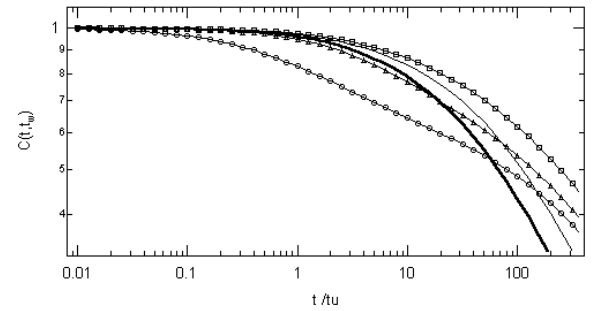


FIG. 9: Same curve that fig5 but for the calculated $C(t_w, t + t_w)$ for $t_w = 0.01tu$ (○), 6 tu (△), 50 tu (□). The amplitude of the strain is $\gamma_0 = 2.5$.

Fig 9 displays $C(t + t_w, t_w)$ for $\gamma_0 = 2.5$ and $t_w = 0.01, 6, 50$ tu after the burst. The reference curves for the unperturbed case at $t_w = 0.01$ -resp 50 tu- are plotted in dark -resp grey- solid lines. For $\gamma_0 = 2.5$, the correlation function $C(t + t_w, t_w)$ for $t_w = 0.01tu$ (○)

starts to decrease before the unperturbed curve. This is a consequence of the overpopulation of low energy states. However, the rate of decorrelation is smaller because the depletion of intermediate energy state. Since the high energies are overpopulated, the two curves crosses. At long time, the unperturbed curve lies under the perturbed one. For longer t_w (\square), the low energy states have aged and the shape of the correlation function is dominated by the population of the high energy. The correlation function for $\gamma_0 = 0.06$ looks 'older' than the reference one. Notice the excellent qualitative agreement between fig 9 and fig 5.

2. effect of frequency

In this section we now focus on the effect of the burst frequency upon the dynamics. We keep the same initial conditions but have ω varying from $2\pi/50$ to 2π . It corresponds to a number of oscillations ranging from 1 to 50. As explained in the previous section we calculated $C(t + t_w, t_w)$ for different t_w after the burst.

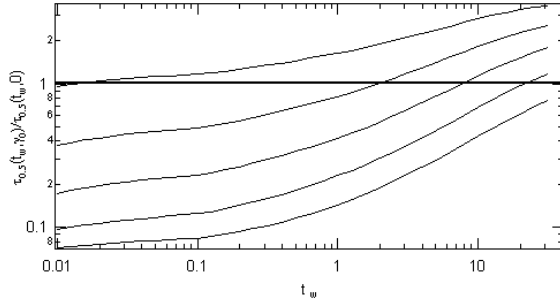


FIG. 10: Calculated $\tau_{0.5}(t_w, \gamma_0) / \tau_{0.5}(t_w, 0)$ for different frequencies of oscillation. The amplitude γ_0 is 10. The frequencies are 0.1Hz, 0.2Hz, 0.3Hz, 0.4Hz, 0.5Hz from bottom to top. Notice that the overaging effect is more sensitive to the frequency for the model than for the experiment.

Following the analysis procedure we used in the experimental section, we define $\tau_{0.5}(t_w, \gamma_0)$ such that $C(\tau_{0.5} + t_w, t_w) = 0.5$. Figure 10 displays $\tau_{0.5}(t_w, \gamma_0)$ as a function of t_w . One can see that it qualitatively predicts the same frequency behavior than that displayed by our sample - see fig 6. Actually oscillatory shear strain, by mixing in strain and thus in ε the population, considerably accelerates the dynamics of the small energy levels, while it does not affect the high energy levels. Thus increasing the frequency $f(t)$ - for the same duration of application - mainly accelerates the low energy dynamics, by making the strain mixing more efficient. Thus the oscillatory strain is qualitatively similar to the square pulse strain. But the amplitude of the splitting in the ε distribution and thus of the overaging considerably increases with the frequency.

C. discussion

We want first to emphasize the following point: overaging is a notion associated with a **transient** perturbation and a comparison with a reference case. It requires not only an analysis of the average relaxation time but of the global shape of $P(\varepsilon, t)$. Overaging comes from the overpopulation of the long relaxation times after the shear application. However, the experiments and the model show that the short relaxation times are simultaneously overpopulated. This is what we called rejuvenation. Because of the simultaneous occurrence of these two phenomena on different time scale, an exact analysis can only be performed if the complete distribution $P(\varepsilon)$ is studied. However, the experimental time window is limited and the system can thus appear rejuvenated or overaged depending on the relaxation times that we can probe. We now wonder if a regime where rejuvenation alone can be achieved for any time scale after a perturbation γ_0 and a duration du . The experiment duration are too limited to give a satisfactory answer. However we can make the following remarks about the SGR model. In this model, aging occurs because for $x < x_g$ the escaping rate $\Gamma_{out}(E)$ is inferior to the entering rate $\Gamma_{in}(E)$ for high enough energy wells. $\Gamma_{out}(E)$ is proportional to $\exp[-E/x]$ and thus depends only on the well's depth. Oppositely, $\Gamma_{in}(E)$ is proportional to $\Gamma(t)$ and thus depends on the whole distribution $P(E)$. Let us first examine the population of the level $(E, 0)$ before the shear such that

$$E \gg E_c = \frac{1}{2} k \gamma_0^2 + x \ln(du)$$

. When a shear is applied, $\Gamma_{out}(E)$ is simply multiplied by a factor $\exp[\frac{1}{2} k l^2 / x]$ during a time du . Hence escaping probability of this population will remain nearly zero despite the shear application. These particles will remain in the states $(E, 0)$ after the shear has been applied. However, for these energies, the entering rate is increased because of the overpopulation of small energies. Overaging comes thus from the fact that the escaping rate remains unchanged whereas the entering rate is increased for large energies. Hence overaging in the SGR model occurs for any finite γ_0 and any finite duration. In this case a complete rejuvenation is impossible. However, the assumption that the trap stiffness is independent of the well depth is only a first step assumption. One could imagine that the deeper the well the stiffer its elastic modulus. One could for instance assume that:

$$k = k_0 + \kappa E$$

where κ is a constant of proportionality. Making this assumption first changes the instantaneous elastic modulus $\langle k \rangle$ of the model. It is no longer k_0 but now

$$\langle k \rangle = k_0 + \kappa \langle E \rangle$$

For $x > x_g$ a stationary distribution of $P(E)$ exists and we find $\langle k \rangle = k_0 + \kappa \frac{x_g x}{x - x_g}$. In the limit of infinite

temperature $\langle k \rangle$ tends towards $k_0 + \kappa x_g$. However, when $x < x_g$, the average energy $\langle E \rangle$ is proportional to $\log(t_w)$ in the asymptotic regime. The instantaneous elastic modulus has thus a logarithmic dependence with the age of the system as observed in many systems [5, 6, 24, 25]. An other change affects the escaping rate. Γ_{out} is now proportional to $\exp[-[\frac{(1-\frac{1}{2}\kappa l^2)}{x}E - \frac{1}{2x}k_0 l^2]]$. The strain now plays a role similar to a temperature change. In this case, the value of E_c now reads:

$$E_c = \frac{\frac{1}{2}k\gamma_0^2 + x \ln(du)}{1 - \frac{1}{2}\kappa\gamma_0^2}$$

One can thus define a critical strain $\gamma_{0c} = \frac{2}{\kappa}$ for which E_c is infinite. Hence a complete rejuvenation can be achieved in a finite amount of time. From an experimental point of view, the distinction between the two approximations by a rejuvenation experiment are not yet concluding. Some other experiments are being performed and the consequences of this modification for the stiffness will be carefully discussed elsewhere.

VI. CONCLUSION

In conclusion, we have shown that an oscillatory strain can act on a glassy colloidal suspension in a dual fashion. It can rejuvenate it by erasing all its past memory. It can also overage it by accelerating the aging process. Both processes comes from an acceleration of the rearrangement rates during a transient time. The dominating effect depends on the amplitude and duration of the shear. We showed that the effect is qualitatively well explained by the SGR model. This model was solved for a realistic strain history. We showed that the distribution of relaxation time was separated into two bumps, one corresponding to rejuvenation and the other one to over-aging. The influence of this two bumps on the position autocorrelation function was studied. We showed that the model and the experiments are highly comparable. We believe that this phenomena is not a special feature of colloidal systems but can be observed in polymer - as indicated by preliminary results performed in our lab - or in spin glasses.

-
- [1] L. Cipelletti, S. Manley, R. Ball, and D. Weitz, Phys.Rev.Lett **84**, 2275 (2000).
 - [2] W. van.Megen, T. Mortensen, and S. Williams, Phys.Rev.E **58**, 6073 (1998).
 - [3] E. Vincent, J. Hammann, M. Ocio, J. Bouchaud, and L. Cugliandolo, *Complex behavior of glassy systems*, vol. 492, springer verlag lecture notes in physics ed., cond-mat/9607224.
 - [4] L. Struik, *Physical Aging in Amorphous Polymers and Other Materials* (Elsevier Scientific Publishing, 1978).
 - [5] C. Derac, A. Ajdari, and F. Lequeux, Euro.Phys.J.E **4**, 355 (2001).
 - [6] M. Cloitre, R. Borrega, and L. Leibler, Phys.Rev.Lett **85**, 4819 (2000).
 - [7] P. Sollich, F. Lequeux, P. Hebraud, and M. Cates, Phys.Rev.Lett **78**, 2020 (1997).
 - [8] S. Fielding, P. Sollich, and M. Cates, J.Rheol **44**, 323 (2000).
 - [9] P. Sollitch, Phys.Rev.E **58**, 738 (1998).
 - [10] W. Hartl, Curr.Opi.Coll.Int.Sci **6**, 479 (2001).
 - [11] R. Larson, *The Structure and Rheology of Complex Fluids* (Oxford University Press, 1999).
 - [12] L. Berthier and J. Bouchaud, cond-mat/0202069 and ref therein.
 - [13] V. Dupuis, E. Vincent, J.-P. Bouchaud, J. Hammann, A. Ito, and H. Aruga Katori, Phys.Rev B **64**, 174204 (2001).
 - [14] L. Bellon, S. Ciliberto, and C. Laroche, Eur.Phys.Jour B **25**, 223 (2002).
 - [15] A. Liu and S. Nagel, Nature **396**, 21 (1998).
 - [16] S. Romer, F. Scheffold, and P. Schurtenberger, Phys.Rev.Lett **85**, 4980 (2000).
 - [17] V. Viasnoff, F. Lequeux, and D. Pine, Rev.Sci.Inst **73**, 2336 (2002). cond-mat/0203396.
 - [18] F. Cardinaux, L. Cipelletti, F. Scheffold, and P. Schurtenberger, Euro.Phys.Lett **57**, 738 (2002).
 - [19] V. Viasnoff and F. Lequeux, Phys.Rev.Lett **89**, 065701 (2002). cond-mat/0203328.
 - [20] C. Monthus and J. Bouchaud, J.Phys. A:Math. Gen, cond-mat/9601012 **29**, 3847 (1996).
 - [21] L. Berthier, private communication.
 - [22] L. Berthier, J. Barrat, and J. Kurchan, Phys.Rev.E **61**, 5464 (2000).
 - [23] D. Durian, D. Weitz, and D. Pine, Science **252**, 686 (1991).
 - [24] D. Bonn, H. Tanaka, C. Wegdam, H. Kellay, and J. Meunier, EuroPhys.Lett **45**, 52 (1998).
 - [25] L. Ramos and L. Cipelletti, Phys.Rev.Lett **87**, 245503 (2001).